THE FUNCTIONAL ROLE OF THE N2B REGION WITHIN THE ELASTIC SARCOMERIC PROTEIN TITIN

By

Joshua James Nedrud

A Thesis Submitted to the Faculty of the

GRADUATE INTERDISCIPLINARY PROGRAM IN
BIOMEDICAL ENGINEERING

In Partial Fulfillment of the Requirements
For the Degree of

MASTER OF SCIENCE

In the Graduate College

THE UNIVERSITY OF ARIZONA

2011

STATEMENT BY AUTHOR

This thesis has been submitted in partial fulfillment of requirements for an advanced degree at The University of Arizona and is deposited in the University Library to be made available to borrowers under rules of the Library.

Brief quotations from this thesis are allowable without special permission, provided that accurate acknowledgment of source is made. Requests for permission for extended quotation from or reproduction of this manuscript in whole or in part may be granted by the head of the major department or the Dean of the Graduate College when in his or her judgment the proposed use of the material is in the interests of scholarship. In all other instances, however, permission must be obtained from the author.

SIGNED: 

APPROVAL BY THESIS DIRECTOR

This thesis has been approved on the date shown below:

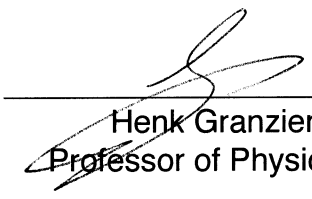

Henk Granzier
Professor of Physiology

04-21-10
Date

TABLE OF CONTENTS

LIST OF ILLUSTRATIONS 4

ABSTRACT 5

INTRODUCTION 6

METHODS 11

RESULTS 19
- Basic Characterization 19
- Biophysical Analysis 22
- Physiological Analysis 26
- Gelsolin Extraction and Oxidative Stress 29
- Cellular Response 34

DISCUSSION 36
- Sources of Hysteresis in the Sarcomere 36
- N2B Removal Increases Hysteresis 42
- N2B Deficiency Affects Slack Sarcomere Length 43
- N2B Removal Induced Energy Loss 44
- Cellular Impact 45

REFERENCES 47

LIST OF ILLUSTRATIONS

Figure 1, Depiction of Sarcomere with Titin Highlighted 7
Figure 2, Heartbeat Protocol 15
Figure 3, Slack Length and Active Tension Changes 20
Figure 4, Passive Tension Changes 21
Figure 5, Triangle Peak Tension Changes 22
Figure 6, Hysteresis Examples 23
Figure 7, Rested Hysteresis 25
Figure 8, Hysteresis Recovery 26
Figure 9, Physiological Hysteresis 28
Figure 10, Gelsolin Extracted Hysteresis 30
Figure 11, Oxidative Stress Response Changes 33
Figure 12, AMPK changes 35
Figure 13, Normalized Hysteresis by Peak Passive Tension 41

ABSTRACT

Utilizing a N2B knockout (KO) mouse model in which the exon that encodes the cardiac-specific N2B unique sequence (N2B-Us) spring element (exon 49) has been deleted, I investigated the mechanical role of the N2B-Us, one of the three extensible regions of cardiac titin. I was able to show that the extensibility provided by the N2B-Us limits energy loss during stretch and shortening cycles of the heart (i.e., during diastole and systole). In a range of conditions, KO mice showed significant increases in hysteresis, a measure of energy loss determined from the area between the stretch and release force-sarcomere length curves, over wild type (WT) mice. Most prominently, hysteresis increased significantly from 320±46 pJ/mm²/sarcomere in WT tissue to 650±94 pJ/mm²/sarcomere in KO tissue that had been preconditioned with a physiological stretch-release protocol ($p < 0.005$). To complement this KO model, oxidative stress was used to mechanically inactivate portions of the N2B-Us of WT titin through cysteine crosslinking. This inactivation displayed a greater increase in hysteresis response in WT compared to KO tissue, (32.3±5% vs. 12.9±2.2%, p-value < 0.05). The results of this study support the concept that the mechanical function of the N2B-Us of titin is to reduce hysteresis and increase the efficiency of the cardiac cycle.

INTRODUCTION

The N2B region is a cardiac-specific extensible element of titin that has been hypothesized to limit energy lost during repeated stretch (diastole)- shortening (systole) cycles of the heart (Helmes et al., 1999). Passive energy loss over each heartbeat arises from differences in energy used to stretch passive restoring force elements and the energy retrieved from these elements as they return the heart to its resting state. This difference in loading and unloading energies is known as hysteresis and causes significant energy loss in passive elements within the sarcomere. In this study I investigated the functional role of the giant filamentous protein titin and its N2B region with respect to hysteresis.

Titin is a major myofilament within the striated muscle's sarcomere. Spanning from the Z-disk to the M-band of the sarcomere (Figure 1), it is the largest known protein in the human body. Titin is oriented along the length of sarcomere, binding to actin of the thin filament in and close to the Z-disk, crossing the I-band free of external binding and then attaching itself along the thick filament, and finally anchoring in the M-band region, which is in the middle of the A-band. The I-band region of titin that is free of external binding is elastic and extends when the sarcomere is elongated and acts as an entropic spring providing restoring force to the sarcomere (Kellermayer et al., 1998). In striated muscle, titin's force

comprises the majority of the passive tension developed by the muscle, with a minor role played by the collagen fibers in the extracellular matrix. This has been shown and is especially true in cardiac muscle over the working sarcomere length range in the heart (Wu et al., 2000).

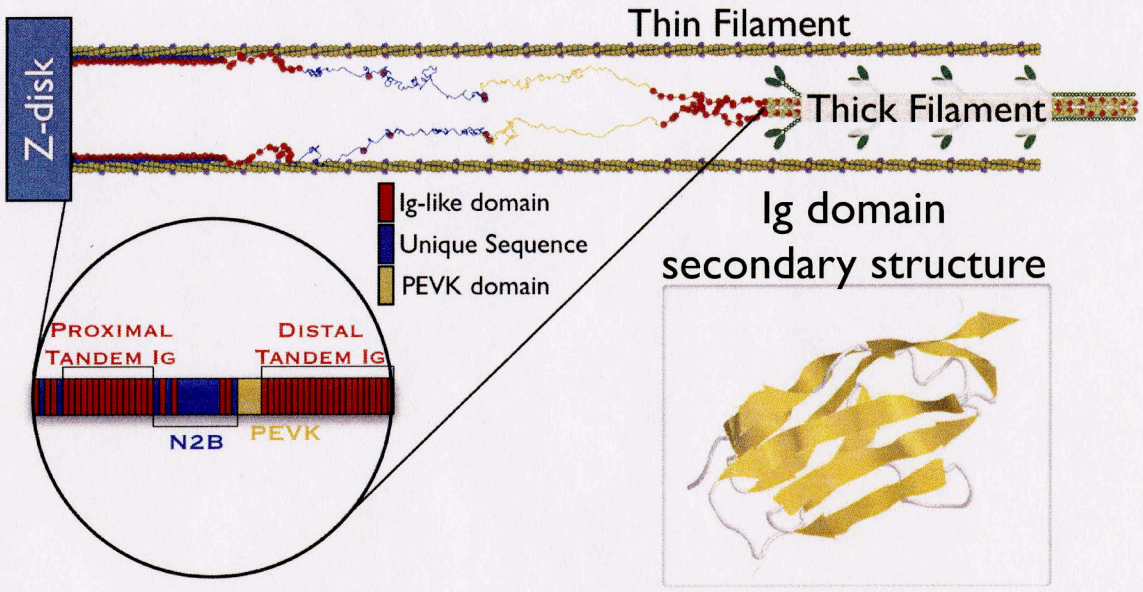

Figure 1
Schematic representation of titin highlighting the extensible I band region. (Top and Left) Cartoon depiction of the I-band of the sarcomere with extensible regions of titin highlighted and labeled. The N2B-Us is a large unique sequence that makes up the majority of the N2B element. (Right) Cartoon rendering of the secondary structure of a single immunoglobulin-like (Ig) domain. Yellow strands highlight the beta barrel structure of this domain.

As shown in Figure 1, titin's extensible I-band region is comprised of three distinct elements: sequentially arranged immunoglobulin-like (Ig-like) domains that comprise the tandem Ig segments, the PEVK element (rich in proline(P), glutamate (E), valine (V), and lysine (K)), and the N2B unique sequence (N2B-

Us) element. In slack sarcomeres, when force is zero, titin's extensible region is in a highly compacted state with a high conformational entropy and sarcomere stretch initially straightens the linker sequences between the tandem Ig domains while the Ig domains themselves remain folded as beta-barrel structures (Improta et al., 1996). Next the N2B-Us and the PEVK region extend, which is thought to be due to straightening of random-coil structures that these sequences form (Helmes et al., 1999). The straightening of titin's extensible region decreases entropy in the molecule, which produces a restoring force against the induced strain, and titin is therefore known as an entropic spring. Each of these regions have different properties and as such are proposed to serve different functions during sarcomeric stretch.

The tandem Ig and PEVK spring element are found in all muscle types, but, interestingly, the N2B spring element is cardiac-specific. Because of the rhythmic activity of the heart, accomplishing 70 beats per min over a life span of 75 years amounting to ~ 3 billion contraction-relaxation cycles over the lifespan of an individual, I hypothesized that cardiac tissue has evolutionarily incorporated the N2B-Us to reduce hysteresis over the cardiac cycle. I tested this hypothesis by using a novel mouse knockout (KO) model in which the N2B element has been excised (N2B KO) (Radke et. al. in 2007). In this work I used a variety of precision mechanical assays to elucidate the increase in hysteresis and possible

changes that the removal of the N2B region brings. I also incorporated a gelsolin thin filament extraction technique in order to differentiate the effect of the N2B-Us on intrinsic titin hysteresis from extrinsic titin hysteresis arising from thin filament-titin interactions and thin-thick filament interactions.

In addition to mechanical assays, I also investigated AMP activated protein kinase (AMPK) and phosphorylated AMPK (AMPK-P) levels to assess the energy status of the myocardium. AMPK, a key energy regulator of the cell, acts by switching off energy consuming processes and activating energy production processes when energy storage levels fall. AMPK is in a perfect position to regulate these processes as it is activated by phosphorylation that occurs with decreased levels of adenosine triphosphate (ATP) and increased levels of adenosine monophosphate (AMP) a byproduct of the release of energy from ATP. Thus AMPK-P is a good indicator of energy load (Carling, 2004). For this reason I measured both AMPK and AMPK-P in wild type (WT) and N2B KO myocardium.

Finally, oxidative conditions were used to induce intermolecular crosslinks within the N2B-Us, creating disulfide bonds between cysteine groups in the sequence. It has been shown in single molecule studies that these links mechanically 'hide' the protein sequences between two linked cysteines, effectively reducing the

contour length, L_c, of the unique sequence (Grützner et al., 2009). Aligning the human N2B-Us used in that study with the mouse N2B-Us (the sequence used in this study), 4 out of the 6 predicted cysteine-bonding pairs are conserved. On average, 242 residues separate the conserved residues; with a maximum residue spacing of 0.38 nm for an unfolded polypeptide (Watanabe et al., 2002), this reduces the L_c of the N2B-Us by 92 nm, a little under half of the 201 nm (530 residues x 0.38 nm) L_c of the N2B-Us in the mouse. It was also confirmed that the PEVK region did not have any cysteines to crosslink, making oxidative crosslinking of the N2B-Us of titin an ideal complement "half KO model" to the genetic N2B full length KO model. Armed with these tools, I set out to elucidate the functional role of the N2B region of titin in reducing energy loss over the cardiac cycle.

METHODS

Preparation of papillary muscles

Murine papillary muscles were harvested from male C57BL/6 N2B 5-month-old knockout (KO) and wild type (WT) mice. All experiments were performed in accordance with the NIH Guide for Care and Use of Laboratory Animals and approved by the IACUC of The University of Arizona. Muscle preparations were dissected as previously described (Lee et al., 2010). Briefly, hearts were rapidly excised and papillary muscles were removed from the left ventricle and skinned in a 1X pCa 9.0 relaxing solution with 1% Triton-X-100 (Pierce, IL, USA) overnight at 4°C. Once lipid bi-layers were fully chemically removed, muscles were thoroughly washed with 1X relaxing solution before being transferred into a 50% (v/v) glycerol to relaxing solution storage solution and stored at -20°C. To prevent protein degradation, all solutions contained protease inhibitors (phenylmethylsulfonyl fluoride (PMSF), 0.5mM; Leupeptin, 0.04mM; E64, 0.01mM).

Mechanics

Skinned muscles were dissected into fiber bundles (0.026±0.001mm² cross sectional area, defined as (width*depth*π/4)) and secured to a servo-motor (Aurora, 308B) and force transducer (Sensor One, AE 801) on either side with

aluminum T-clips. Muscles were set to slack length, defined as sarcomere length with zero passive stress, and fiber lengths were recorded through a calibrated video monitor. Tension and sarcomere length (SL) were recorded simultaneously with the force transducer and a calibrated laser diffraction system through a 16-bit DAQ board (National Instruments, PCI-6036E) into custom-made labview software. Active tension was used as measure of skinned tissue health by activating the skinned fibers with pCa 4.0 activating solution (BES 40 mM, $CaCO_3$-EGTA 10 mM, $MgCl_2$ 6.29 mM, Na-ATP 6.12 mM, DTT 1 mM, K-propionate 45.3 mM, creatine phosphate 15 mM, pH 7.0). Initially total passive tension was measured with a variety of mechanical protocols used to probe the passive energetic differences between WT and KO skinned tissue, these are described in detail below. After total passive tension had been collected, high molar KCl and KI solutions were used to depolymerize thick and thin filaments respectively, thereby removing anchoring sites for titin (Granzier and Irving, 1995). With anchoring sites for titin removed, titin no longer contributes to passive tension within the sarcomere, and the remaining passive forces are mainly attributed to the extracellular matrix (ECM), primarily collagen. By subtracting the extraction insensitive tensions from total tension, extraction sensitive tension was calculated, which is attributed to titin. All passive tensions reported in this thesis have extraction insensitive portions subtracted and only report titin forces unless noted.

Four different mechanical protocols were run over the course of collecting data for this publication. For each protocol the slack SL was determined by recording the SL at the point where any buckle in the tissue was taken out, the tissue looked visually straight, and no force had been built up yet. After slack length had been determined, the tissue was briefly activated as described above and allowed to rest afterward for a minimum of 10 minutes in relaxing solution. Once fully rested, slack SL was confirmed and a series of small stretches to 5, 10, and 15% of baseline length were imposed on the tissue to form a strain-SL relationship. This calibration was used in calculating strains needed for later stretches and at this point a series of stretches specific for each protocol were run.

The first protocol consisted of a combination of single triangle stretches from slack to specified SLs (2.1, 2.2, 2.3μm) at each of three different strain rates (0.1, 1, 10 lengths/sec), for a total of 9 stretches. These stretches were used to evaluate passive tension development and hysteresis of rested muscle. Between each stretch a period of rest was allotted (a minimum of 5 minutes, with longer rest periods for larger stretches) to allow the tissue to fully recover so as not to affect results of the following stretches. A second protocol evaluated the time it takes to fully recover from the imposed strain. For these stretches a rested

muscle was stretched from slack to 2.2μm at 10%/s. After this stretch the tissue was returned to slack at 1000%/s and allowed to rest for a period between 0 to 120 seconds. After resting a set amount of time a second triangle stretch from slack to 2.2μm was performed to evaluate recovery progression. After each stretch pair the tissue was allowed to rest for 20 minutes to ensure full recovery before evaluating recovery again. As a further precaution against previous stretches affecting recovery time for subsequent stretches, the order of stretches were randomized every few tissues.

A third protocol was developed to look at passive tension development and hysteresis that closely mimicked the cardiac cycle. In this protocol a series of tandem triangle stretches from slack to a SL of 2.2μm at 3 lengths per second (this combination of stretch amplitude and stretch speed provides a cyclical rate of 600 beats per minute) were repeated up to 12000 cycles to evaluate tissue preconditioning and hysteresis that closely resemble the cardiac cycle (Chung and Granzier, 2011). A fourth protocol was developed that incorporated the constant cycling pattern of the above protocol, but approximated the stretch pattern of a heartbeat. Diastolic filling was approximated by a longer 0.055 sec ramp stretch from slack to 2.2μm followed by an approximation of the isovolumetric contraction phase where the muscle tissue was held at 2.2μm for 0.005sec. The ejection phase was approximated by a faster 0.035 sec downward

ramp to slack and finally followed by an isovolumetric relaxation phase by holding at slack for 0.005sec (Figure 2). Timings were approximated from doppler echocardiography and scaled for 600 beats per minute; physiological heart beat of a conscious mouse (Noujaim et al., 2004). This pattern was repeated a minimum of 1000 cycles to ensure full preconditioning.

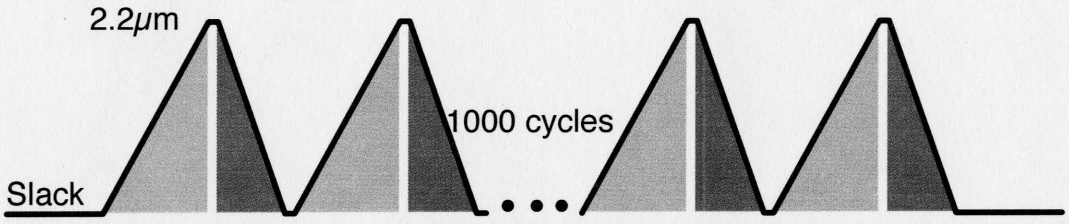

Figure 2
Heartbeat stretching protocol, the light grey fill indicates diastolic filling, the dark grey fill indicates ejection. Interstitial periods represent isovolumic periods within the heartbeat cycle.

Western Blot Analysis

Freshly frozen left ventricular (LV) heart samples were solubilized and proteins were separated by 8% SDS-PAGE electrophoresis and then transferred to PVDF blotting membrane (Immobilon-FL, Millipore, USA) using a trans-blot SD semi dry transfer cell (Bio-Rad, CA, USA) at a current of 165 mA for 1.2 hrs. The membranes were stained with Ponceau S (Sigma) to visualize total proteins and scanned (Epson 800 scanner). Primary antibodies anti-AMPKα and anti-phospho-AMPKα (raised in rabbit, Cell Signaling, catalog #s: 2532 and 2531) were diluted 1:1000 in blocking solution containing 0.05% Tween 20, 50% blocking buffer (Odyssey), 50% PBS pH 7.5. The membranes were incubated

overnight on a shaker. Secondary fluorescent antibody CF680 goat anti-rabbit (Biotum) was diluted 1:20000 in 0.02% SDS, 0.05% Tween 20, 50% blocking buffer, 50% PBS pH 7.5. The membranes were incubated 1h at RT on a shaker. The membranes were scanned for infrared fluorescent detection (Odyssey Infrared Imaging System, Li-Cor Biosciences). All WB data was normalized by the protein loading.

Thin filament extraction with gelsolin

I also studied tissue from which the thin filaments had been extracted in order to isolate the role of titin from the thin filament. Utilizing skinned fiber preparations, as described above, thin filaments were extracted with a calcium independent gelsolin fragment (amino acids 1–406; dissolved in 10 mM 3-(N-morpholino) propanesulfonic acid (MOPS), 1.0 mM EGTA, 1.0 mM Mg-acetate, 20 mM K-propionate, 1 mM DTT, and 20 µg/ml leupeptin, pH 7.0 at 21–23 °C) (Granzier et al., 1997). Tissue was incubated and rocked gently in a gelsolin (1 µg/µl) cocktail (20 µl gelsolin: 20 µl ddH2O: 40 µl 2X relaxing solution) overnight at 4 °C for 12 hrs. The extracted tissue was then rinsed at room temperature for an hour in relaxing solution. Following gelsolin extraction, maximal active tension was recorded to ensure proper thin filament extraction. WT and KO tissue had similar active tension after gelsolin extraction; overall post extraction tension was 4.4±1.5% of un-extracted maximal tension indicating nearly full thin filament

extraction. Upon extraction, the tissue was mechanically examined with tandem triangle stretches as described above.

Oxidative Stress

For these experiments I used gelsolin treated skinned muscle as described above. The removal of thin filaments was used to preclude crosslinking between actin and either myosin or titin during induced oxidative states. After gelsolin extraction, tandem triangle stretches from slack to 2.2μm at 600 cycles/minute were imposed on the tissue while SL and tension were recorded as described above. Initially preparations were bathed in regular relaxing solution for the first 10 minutes of mechanical perturbations. Once fully preconditioned, the bath solution was switched out with reductase free relaxing solution, relaxing solution with 0mM DTT, in preparation for the addition of 5mM hydrogen peroxide. During stretch cycles, 5mM H_2O_2 relaxing solution was then washed in and peak tension was monitored for up to 1hour afterward to evaluate sufficient time for full crosslinking. After sufficient time for crosslinking, the 5mM H_2O_2 relaxing solution was washed out and replaced with DTT free relaxing solution in order to remove any possible side effects the hydrogen peroxide itself may have on passive tension, for which none were found. Finally, 10mM DTT relaxing solution was used to remove formed crosslinks, and then replaced with regular relaxing

solution to assure complete reversal and preclude any complications from the higher concentration of DTT used to dissociate the crosslinking.

Calculations

Hysteresis values were calculated in a custom Ruby program with a bridge to Matlab, where area under the loading and unloading curves were totaled with trapezoidal integration using the *trapz* subroutine.

Time constants values for recovery experiments were calculated by fitting a rising exponential equation to the recovery percentages plotted against rest time. In this model, "a" is the amplitude of the recovery, "Δt" is the rest time between the initial and secondary stretch, "y_o" is the baseline hysteresis recover at no rest time, "τ" is the resultant time constant of the equation.

$$Recovery = a(1 - e^{-\Delta t * \tau}) + y_o$$

Statistics

Data are presented as mean ± SE. Significant differences were probed using student's t-test. Probability values < 0.05 were taken as significant.

RESULTS

Basic characterization

To establish the functional role(s) of the cardiac-specific N2B element, especially its role in hysteresis, I mechanically characterized the passive properties of skinned papillary muscles isolated from the N2B KO mouse model and compared results to those of age and gender matched WT mice. I first measured the maximal active tension (pCa 4.0) at a SL of 2.0 μm and found that the KO and WT myocardium generate similar active stress levels: 47.9±3.7 mN/mm^2 (KO) vs. 41.5±2.9 mN/mm^2 (WT) (Figure 3A). The slack SL was established both before and after activation by shortening the passive muscle until it clearly buckled, holding it there for 10 min, and then stretching the muscle to the minimal length at which the buckle was taken up and where no detectable passive force was developed, at which point the sarcomere length was measured by laser diffraction. Consistent with previous work on N2B KO single cardiac myocytes the slack SL was significantly shorter in KO than WT muscle (1.86±0.01 μm (KO) vs.1.89±0.01 μm (WT), p-value: <0.001). The observed WT slack SL was similar to that previously measured for WT isolated myocytes (1.90 μm ± 0.002). However, the slack SL for my KO skinned bundles, again 1.86±0.01 μm, were considerably longer than that recorded from previous N2B KO intact myocytes experiments (1.80 ±0.01 μm) (Radke et al., 2007). This discrepancy may arise

because intact myocytes experience a low level of active tension during diastole, which compresses the cell compared to the uncompressed SL in a mechanical slack model (King et al. 2007).

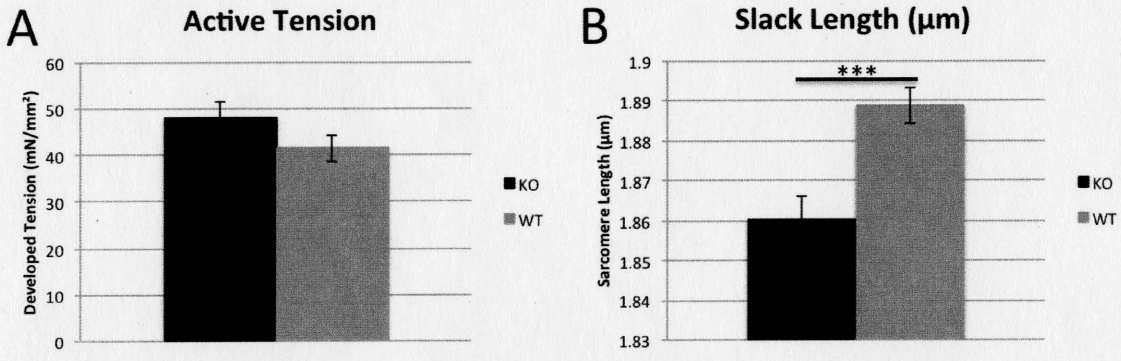

Figure 3

(A) Average active developed tension, KO and WT data sets were not significantly different from each other, both developing active tension within the range of published results for skinned mouse papillary muscle (Lee et al., 2010; Wu et al., 2000; Kirk et al., 2009; Vahebi et al., 2005). (B) Average resting slack length of KO and WT tissue with standard error bars. KO tissue had a significantly smaller slack length compared to WT tissue. (p-value < 0.001)

The basic passive tension-SL relation was characterized by stretching rested muscle from its slack length to a final SL of 2.3 μm with a velocity of 0.1 lengths/sec in relaxing solution. Total, KCl/KI extraction insensitive (primarily ECM), and KCl/KI extraction sensitive (primarily titin) passive tensions were calculated (see Methods for details) and are shown in Figure 4. Although the ECM-based passive tension trended higher at longer SL in N2B KO compared to WT tissue, the difference did not reach significance. Titin-based passive tension, on the other hand, was significantly higher in KO tissue, and at SL of 2.3 μm,

developed 41.8±6.8 mN/mm² of passive tension vs. 8.5±0.8 mN/mm² in WT (p-value <0.001) (Figure 4). Dividing titin tension by total tension, the percent contribution of titin was evaluated. Because of the small signal to noise ratio in force measurements at short sarcomere lengths, titin contribution was only calculated for SL values greater than 2.0 μm. Titin contribution to total passive tension was found to be significantly greater in KO compared to WT tissue at SL < 2.2μm (Figure 4 inset). After SL 2.2μm, WT and KO differ less and are no longer statistically significant different. This is explained by the jump in contribution of the ECM, primarily collagen, after SL 2.2μm.

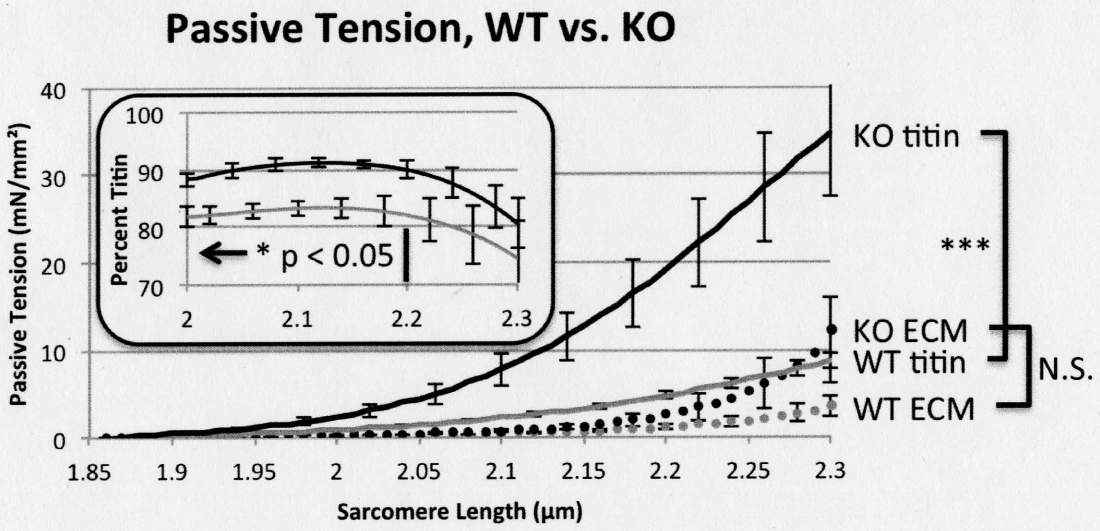

Figure 4
Average passive tension curves for collagen and titin with standard error bars. While collagen passive tension is slightly elevated in N2B KO mice, this increase is not significant over the working distance of the stretch (P > 0.1). Titin tension is significantly increased with P < 0.05 at sarcomere lengths ≥ 1.9 μm. (Inset) Average percent titin contribution to total tension. Percent

contribution by N2B KO tissue is significantly increased ($P < 0.05$) at sarcomere lengths ≤ 2.2μm.

Biophysical Analysis

As a first step in evaluating the passive energetic changes due to modification of titin through removal of its N2B region, I measured titin passive tension by stretching rested fiber bundles from slack to 3 different SLs (2.1, 2.2, and 2.3 μm) at 3 different speeds varied by 2 orders of magnitude (0.1, 1, 10 lengths/second). Peak passive tension was significantly larger in the KO compared to WT tissue in all 9 stretch patterns (Figure 5).

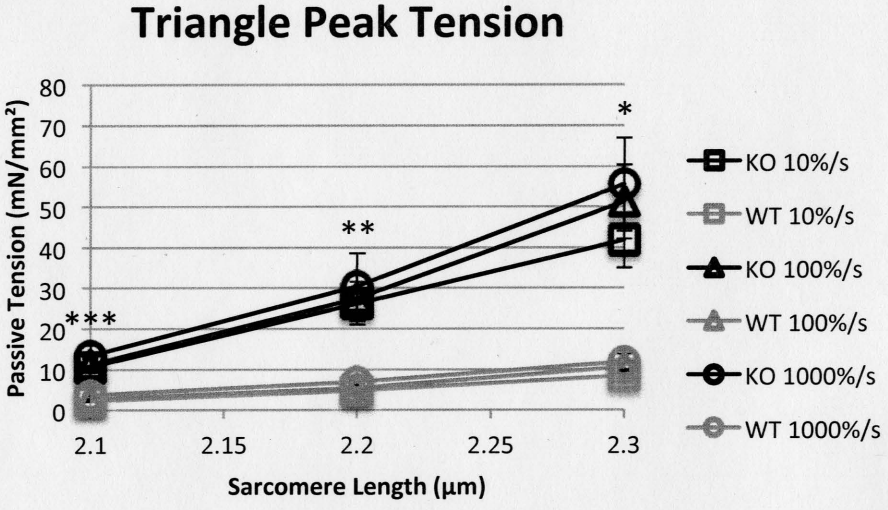

Figure 5
Peak titin tension was significantly higher in skinned muscle fibers of N2B-KO mice at every speed when stretched from rest at slack to every sarcomere length tested, under a single triangle stretch protocol. (p-value legend: * < 0.05, ** < 0.01, *** < 0.005 between WT and KO at all matching speeds).

In addition to analyzing peak passive tension for these 9 stretch patterns, hysteresis was also calculated. In mechanical terms, hysteresis is defined as the circular integral of tension over position. I quantified this value by integrating the area between the tension-SL curves. Using a symmetrical stretch-release protocol (Figure 6 inset, upper), loading and unloading curves were measured (Figure 6 inset, lower) and used to calculated hysteresis (Figure 6).

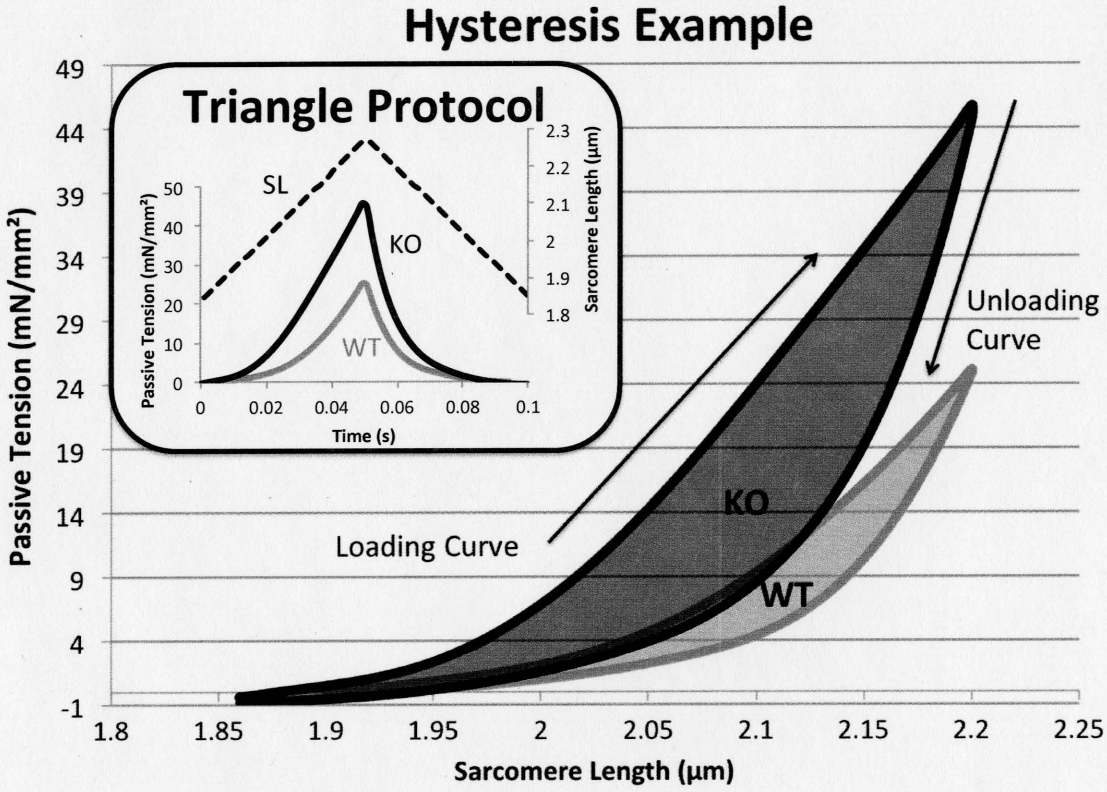

Figure 6

(Inset) top, dashed black line shows imposed sarcomere length change over time; lower, example tension traces over time for both WT and KO tissue, light and dark grey respectively. (Main) Example of WT and KO hysteresis. Hysteresis is the area between the loading and unloading curves, highlighted in the figure by a gray scale fill between the two curves.

Using the same stretch data as above, hysteresis was calculated and found to be significantly larger in KO compared to WT muscles at all SL and strain rate combinations (Figure 7). For example, at a strain rate of 1.0 length/s to a SL of 2.2μm, hysteresis was 1.08±0.24 nJ/mm²/sarcomere in KO and 0.22±0.02 nJ/mm²/sarcomere in WT (p-value < 0.01).

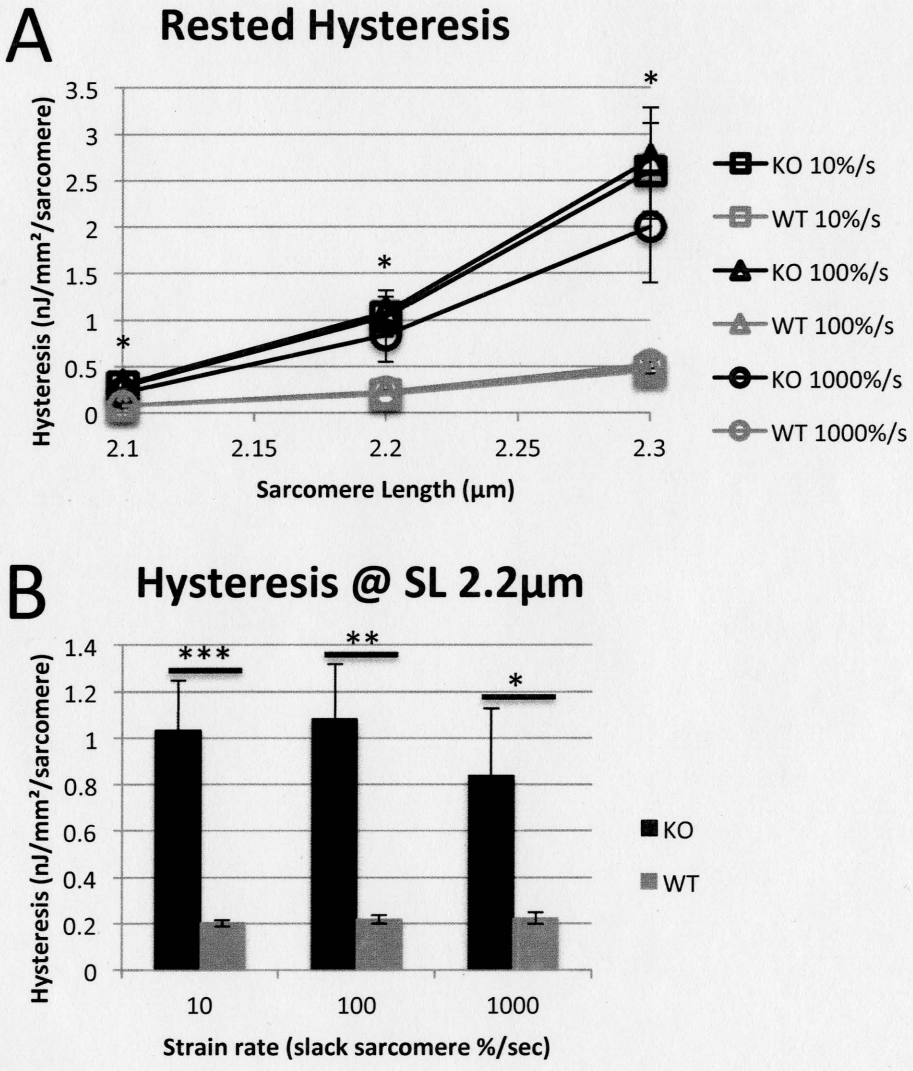

Figure 7

(A) Titin hysteresis (energy loss during stretch-release cycle) increased significantly in skinned muscle fibers of N2B-KO mice at every speed when stretched from rest at slack to every sarcomere length tested, under a single triangle stretch protocol. (p-value legend: * < 0.05, *** < 0.005) (B) A bar graph showing hysteresis differences between WT and KO tissue over triangle stretches from slack to 2.2μm at a variety of stretch speeds (p-value legend: * < 0.05, *** < 0.005).

To evaluate whether similar processes underlie hysteresis in WT and KO muscle, I also studied hysteresis recovery. Muscles were stretched from slack length to 2.2µm at 0.1 lengths per second followed by a release back to the original length at 10 lengths per second, releasing in about 10 milliseconds. Following a rest period a second stretch was performed at 0.1 lengths per second to a SL of 2.2μm (Figure 8A). The force-sarcomere trace was similar for long rest periods (>30s) but differed substantially at short rest periods (<~10s). The difference was quantified as percent recovery by dividing the area under the loading curve of the second stretch by that of the initial stretch (Figure 8). Time constants of 0.24 s^{-1} and 0.15 s^{-1}, WT and KO respectively, were derived from a single exponential time relationship (see methods) fit with a nonlinear least-squares method (Nelder-Mead simplex algorithm). No significant differences were found between WT and KO muscles.

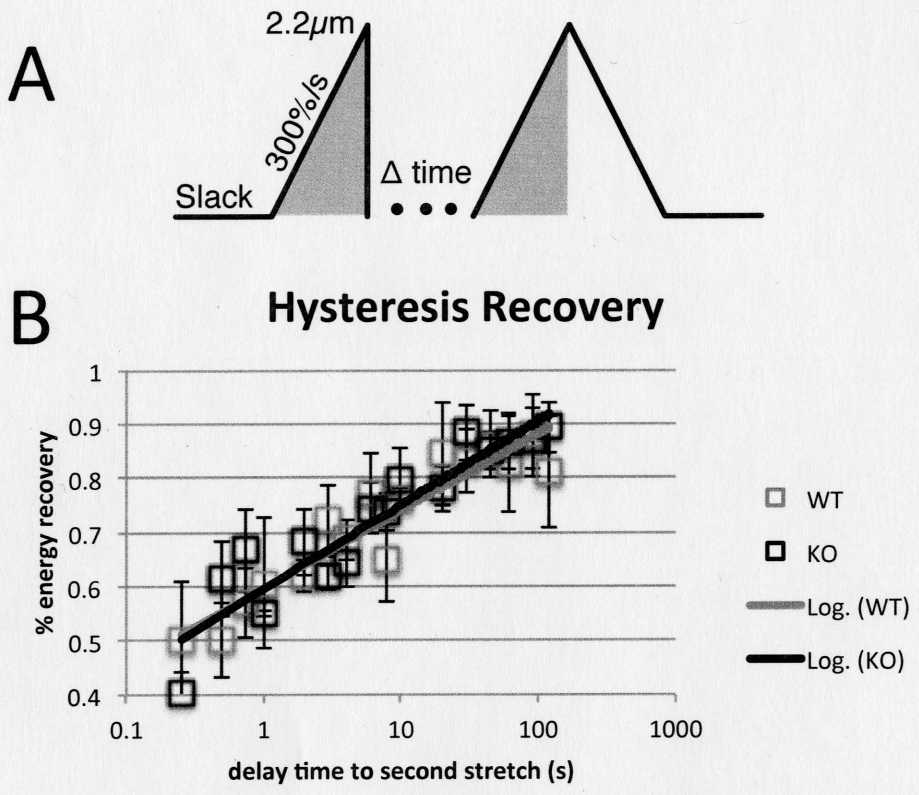

Figure 8

(A) Hysteresis recovery protocol. After an initial stretch to SL 2.2μm at 300%/s, the preparation was immediately returned to slack length and allowed to rest at slack for a variable amount of time. After this rest period, a second stretch with the same characterizations as the first. (B) Recovery with respect to rest time did not show a differentiation between KO and WT tissue. Thick lines show a log line of best fit through the aggregate data.

Physiological Analysis

All results shown above were obtained by stretching muscles that had been rested at their slack length for >5 min. This is very different from the situation in the living mouse where titin is continuously stretch-released in rapid succession at a rate of 600 beats per min. In order to more accurately represent physiology,

a repeated stretch-release protocol was used with no rest in between cycles. I stretched from slack SL to 2.2 μm and used a speed of 3 lengths/second, approximating physiological conditions. In both WT and KO tissue, hysteresis was found to be highest in the first stretch-release cycle, then rapidly decrease during the subsequent 5 cycles and to reach an approximate steady value after ~200 cycles (Figure 9B). Hysteresis started off much higher in the KO tissue and leveled off at a significantly higher level as well. After 200 cycles hysteresis was 650±94 pJ/mm²/sarcomere in KO and 320±46 pJ/mm²/sarcomere in WT muscle (p-value 0.02). A second set of stretches was conducted after a 20-minute rest at slack and the tissue was shown to fully recover both peak tension and hysteresis development (results not shown). This indicates that the decay in hysteresis and passive tension during the repeated stretches is a normal and physiological mechanism and previous stretches did not induce structural damage to the sarcomere.

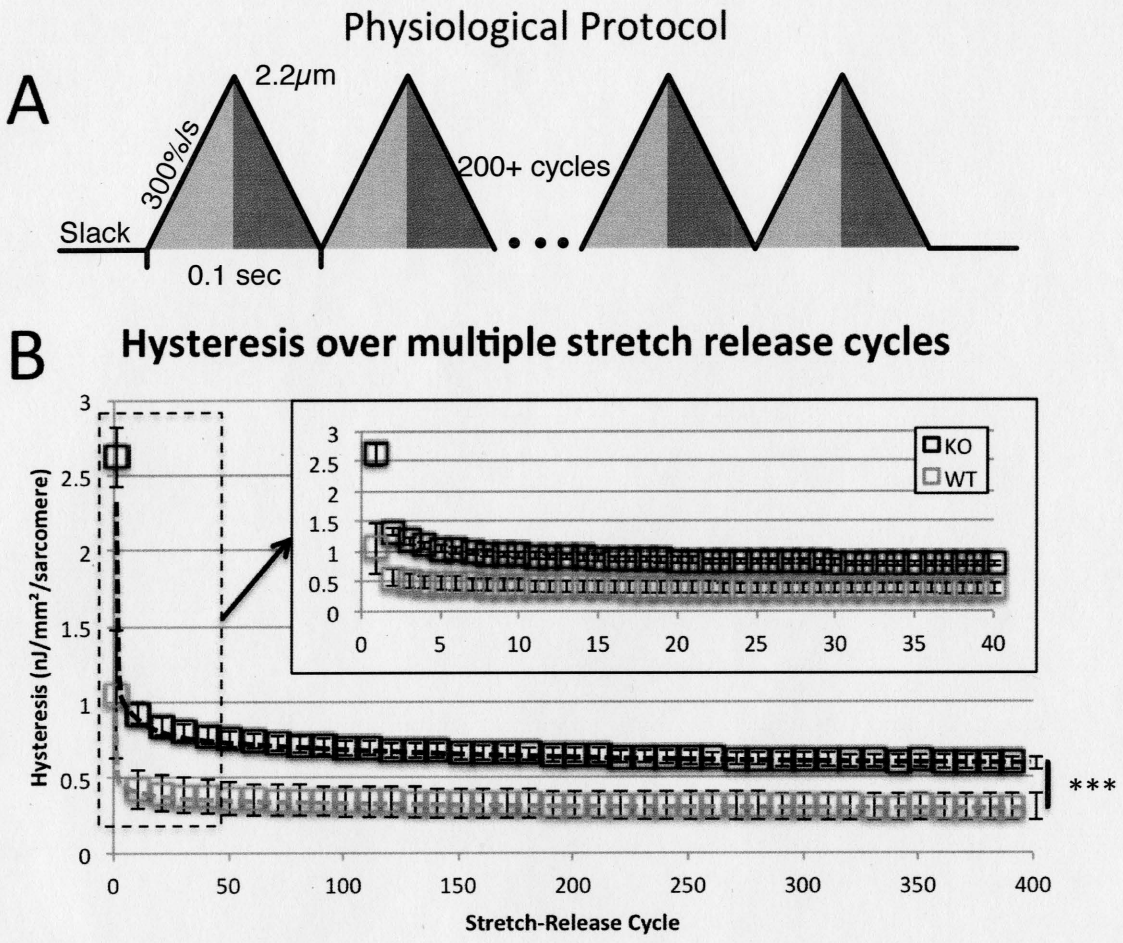

Figure 9

(A) Physiological stretching protocol. Triangle stretch patterns were repeated multiple times in tandem in order to simulate the cyclical loading of the heart. These stretches imposed a displacement from slack to 2.2μm at a rate of ~10Hz. Light grey filling denotes the loading curve, while dark grey filling denotes the unloading curve. (B) Titin hysteresis decay over cycle count during a repeated conditioning protocol. Passive hysteresis is elevated significantly in skinned muscle fibers of N2B-KO mice at all cycles. (average t-test p-value: 0.014) Main graph, every 10th cycle is shown up to 400 cycles. Inset, the first 40 cycles are shown (p-value *** < 0.005).

I also imposed a protocol that even more accurately represents physiology by mimicking isovolumic relaxation, filling, isovolumic contraction, and ejection phases (See methods for full details). No significant differences were found between this protocol and the simpler triangle stretches (results not shown). Because of this, along with the ease of implementing and analyzing triangle stretches, their continued use is seen in the rest of this study.

Gelsolin Extraction and Oxidative Stress

To elucidate the contribution of interfilament viscosity to hysteresis, a series of gelsolin extraction experiments were conducted. Gelsolin, a filamentous actin severing protein (Granzier et al., 1997), facilitates dissociation and removal of the actin-comprised thin filaments and thereby removes potential interactions between the thin and thick filament as well as thin filament and titin. By removing these potential interactions I was able to isolate passive stress and hysteresis intrinsic to titin. To ensure proper thin filament extraction, I activated the tissue with a pCa^{2+} 4.0 activating solution. WT and KO tissue had similar active tension after gelsolin extraction; overall post extraction tension was 4.4±1.5% of un-extracted maximal tension indicating nearly full thin filament extraction. I tested both gelsolin extracted WT and KO muscle against their respective genotype matched non-gelsolin extracted controls with the triangle physiological stretch described previously (Figure 9A). The removal of the thin filaments reduced initial

and steady state peak passive tensions equally, ~50% compared to non-gelsolin extracted control muscle for both WT and KO tissue. (Figure 10A). Hysteresis, on the other hand, was greatly reduced the initial rested triangle stretch by 60%, but differed by only 25% at steady state, again, this was consistent in both WT and KO tissue. (Figure 10B).

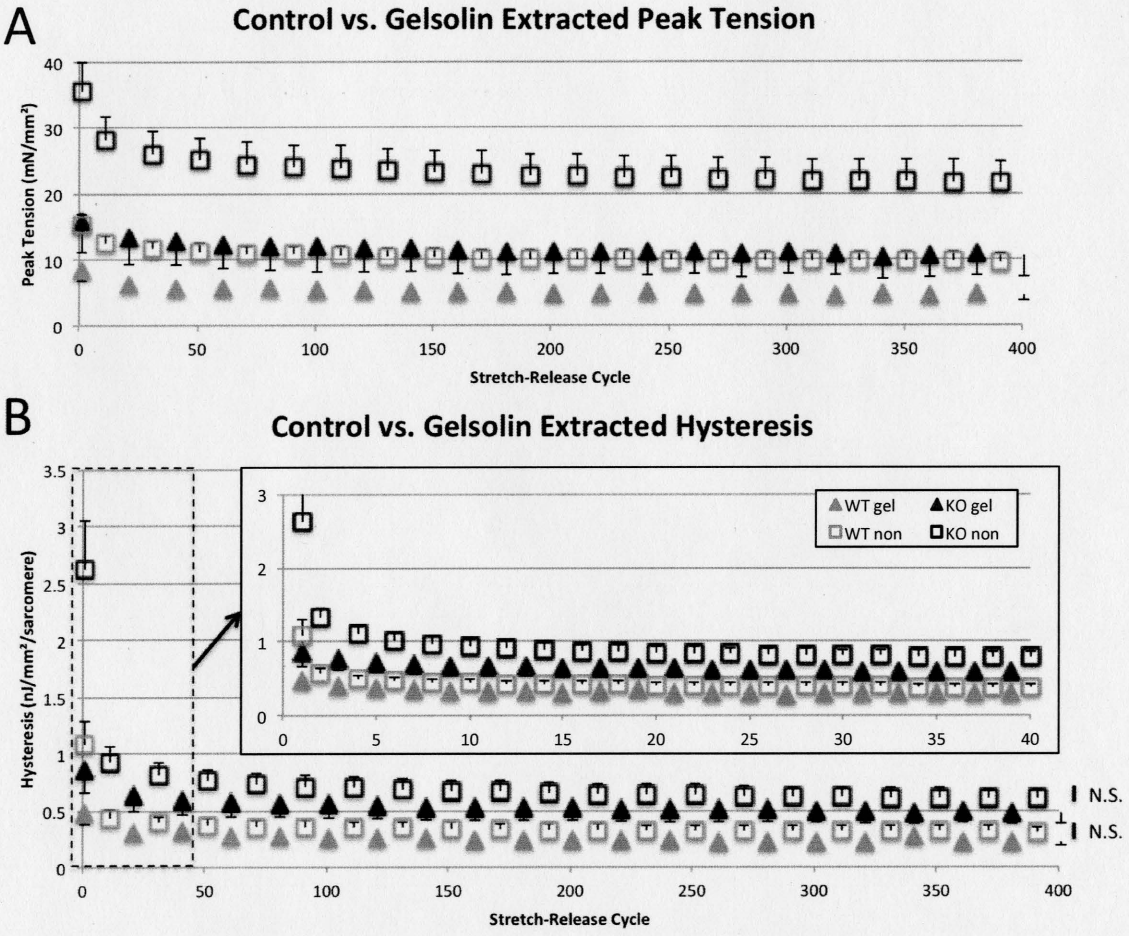

Figure 10

Peak passive tension (A) and hysteresis (B) of thin-filament extracted skinned muscle under physiological strain patterns compared to non-gelsolin extracted tissue. WT tissue is shown in grey, KO tissue is shown in black. Gelsolin-extracted tissue is indicated by filled in triangles while control (non-gelsolin extracted)

tissue is shown by non-filled square boxes. For the larger graphs, every 20th point is shown with gelsolin extracted points offset by 10 cycles. The inset graph in B shows every other point with gelsolin extracted points offset by one cycle. (A) Peak passive tension is decreased fractionally by ~50% throughout preconditioning in both WT and KO tissue (B) Hysteresis is greatly decreased (~60%) for the initial triangle stretch in gelsolin-extracted rested muscle compared to genotype matched controls. However, this difference quickly diminishes and steady state hysteresis values are only decreased by ~25% upon preconditioning.

Because genetic models always have the potential that adaptive responses may cause spurious effects and impact the results of interest, I decided to test the effect of reduced N2B-Us compliance on hysteresis using an alternative approach. Because the large unique sequence that comprises the extensible region of the N2B element contains cysteine residues that form disulfide cross bridges under oxidative states (Grützner et al., 2009), these crosslinks functionally 'hide' part of the N2B-Us by removing the spring-like properties of the amino-acids between the two cysteines. Thus, I tested whether oxidizing the N2B-Us in WT tissue results in WT tissue that will display partial KO-like properties. Oxidative states were induced in WT and KO tissue while undergoing the physiological stretch-release protocol. Before oxidative conditions were induced, thin filaments were extracted with gelsolin to minimize mechanically pertinent crosslinks other than in the N2B-Us, for instance myosin crosslinks to actin or titin crosslinks to the thin filament. After thin filament extraction 5mM hydrogen peroxide was added to the relaxing solution to induce oxidative

conditions. This concentration was used to ensure maximal crosslinking in a reasonable amount of time and is within values used to induce oxidative states in other studies (Slezak et al., 1995; Avner et al., 2010; Janero and Hreniuk, 1991). After hydrogen peroxide was added, peak passive tension was monitored for one hour, over which, oxidative cross-linking was found to occur within ~ 20 min. After complete crosslinking, hydrogen peroxide was washed out and replaced with relaxing solution free of reductases (0mM DTT) in order to remove any possible effects arising from the H_2O_2 itself, for which none were found (Figure 11). The results from induced oxidative stress show a significantly larger percent passive tension increase in WT tissue, 40.4±4.9%, compared to KO tissue, 10.5±3.7%, p-value < 0.005. Similarly, the percent increase in hysteresis response was 32.3±5% in WT tissue, which is significantly greater than the percent increase seen in KO tissue, 12.9±2.2%, p-value < 0.05. Both peak tension and hysteresis returned to pre H_2O_2 levels in WT and KO tissue after the addition of 10mM DTT, a potent reductase, showing the reversibility of this effect.

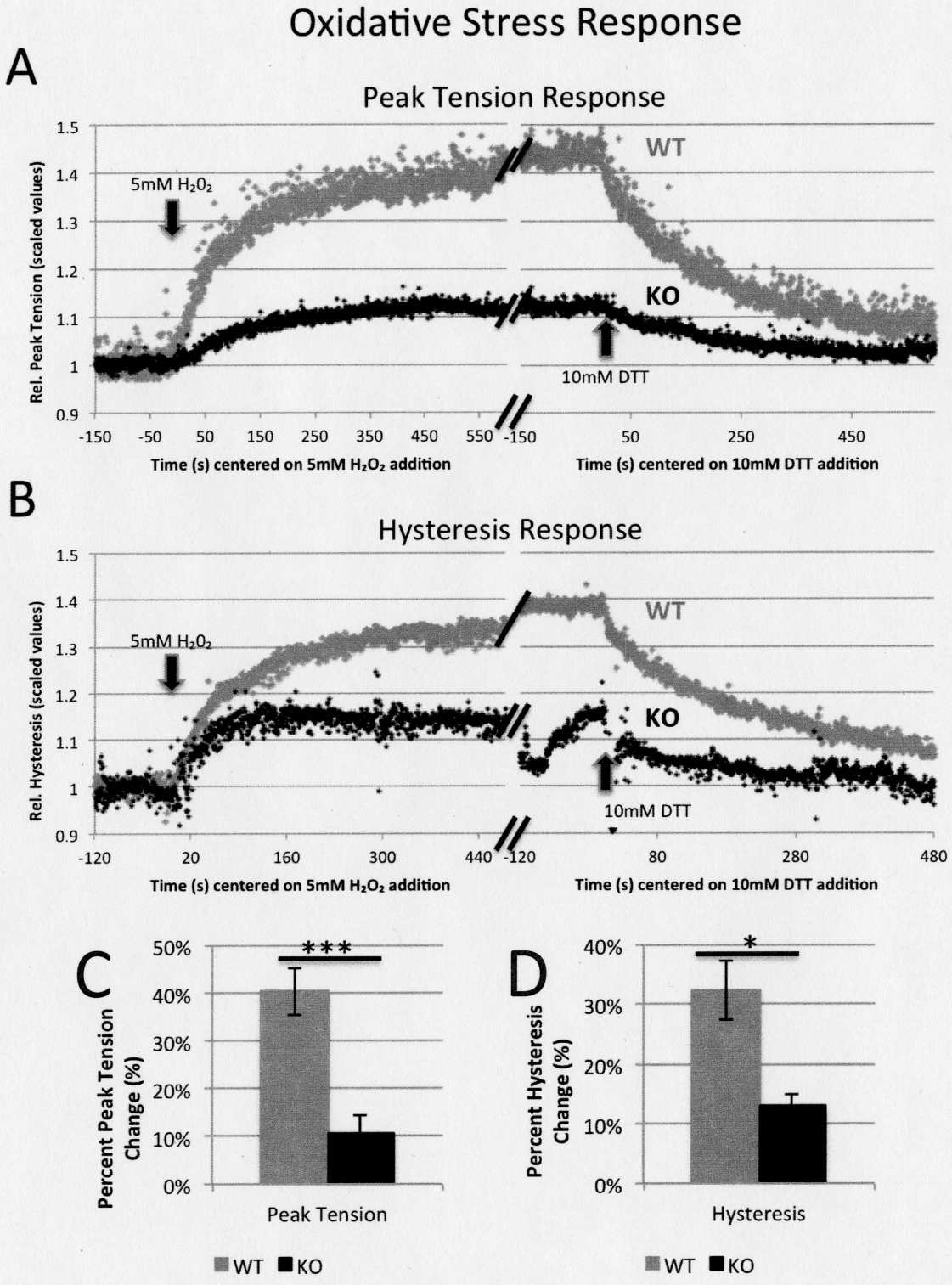
Oxidative Stress Response
A
Peak Tension Response
Rel. Peak Tension (scaled values)
1.5
1.4
1.3
1.2
1.1
1
0.9
5mM H_2O_2
WT
KO
10mM DTT
-150 -50 50 150 250 350 450 550 -150 50 250 450
Time (s) centered on 5mM H_2O_2 addition
Time (s) centered on 10mM DTT addition
B
Hysteresis Response
Rel. Hysteresis (scaled values)
1.5
1.4
1.3
1.2
1.1
1
0.9
5mM H_2O_2
WT
KO
10mM DTT
-120 20 160 300 440 -120 80 280 480
Time (s) centered on 5mM H_2O_2 addition
Time (s) centered on 10mM DTT addition
C
Percent Peak Tension Change (%)
50%
40%
30%
20%
10%
0%
***
Peak Tension
WT KO
D
Percent Hysteresis Change (%)
40%
30%
20%
10%
0%
*
Hysteresis
WT KO

Figure 11

Oxidative stress response while using a physiological cyclical loading pattern (see figure 9A for details). All values are reported in relative changes to the steady state values after 20 min of stretching. When the tissue had been fully preconditioned 5mM hydrogen peroxide was added at the first arrow, at which time disulfide bonding can form in the N2B-Us. After maximal crosslinking has occurred the hydrogen peroxide was washed out and 10mM DTT was added (second arrow), reversing the oxidative response. (A) Example curves of peak tension generation during stretching (B) Hysteresis response example curves. (C) A bar graph depiction showing the relative increases in peak passive tension due to oxidative conditions. KO tissue has a significantly smaller relative increase in passive tension compared to WT, as the KO lacks an N2B region. (p-value *** < 0.005) (D) A bar graph showing the relative increase in hysteresis due to oxidative conditions. As in peak passive tension KO tissue has a significantly smaller relative increase in hysteresis compared to WT. (p-value * < 0.05).

Cellular Response

Because these results revealed that energy loss in the N2B-Us deficient muscle is much larger than in the WT muscle, I asked myself whether this is reflected in the AMPK and AMPK-P levels, both of which are seen as cellular markers for energetic stress. AMPK is a key indicator molecule for energy load on a cell, sensing the relative concentrations of AMP and ATP the main energy storage molecule in the cell. With connections to many metabolic processes and the ability to allosterically interact with AMP, cells will activate AMPK through phosphorylation during times of stress or starvation to decrease energy consuming metabolic activity and increase energy production pathways (Wijesekara et al., 2010). Western Blot analysis was used to quantify AMPK and

AMPK-P. In the KO solubiliations, both AMPK and AMPK-P sets had one data point that stood apart from the others, yet was not statistically an outlier. This increased the variance of my data to a range outside statistical significance.

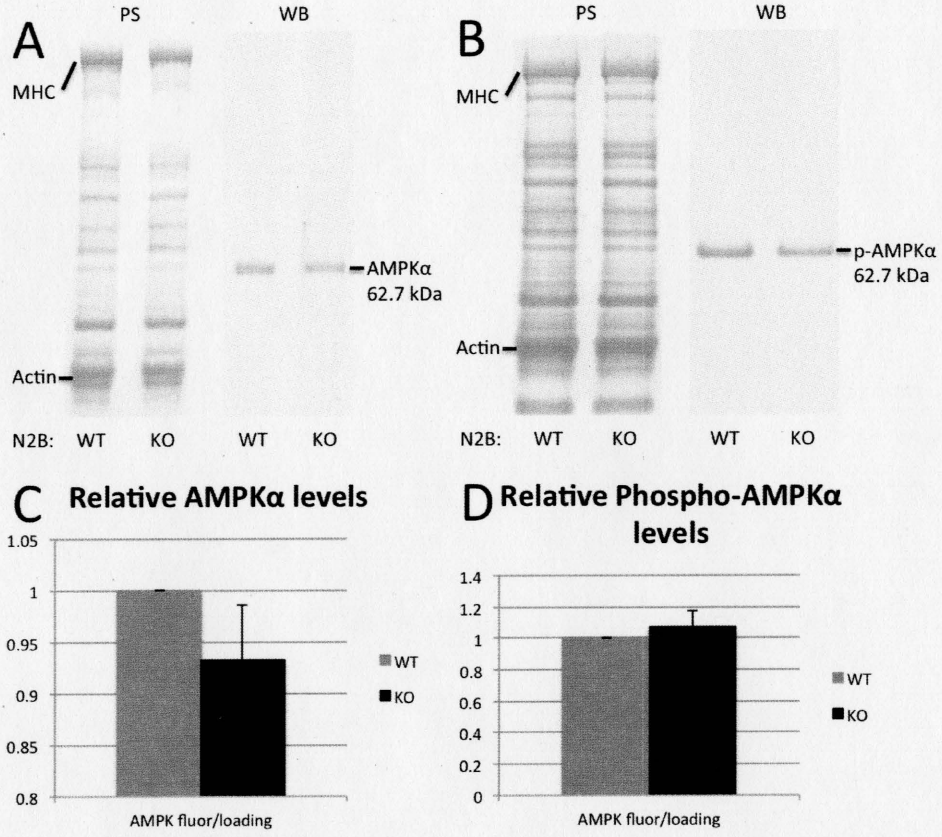

Figure 12

(A) AMPKα example gel, left Ponceau-S total protein membrane stain, right western blot antibody tagged fluorescent signal (B) phospho-AMPKα example gel. (C) Relative AMPKα protein concentrations, a key indicator of metabolic stress, in WT and KO left ventricle wall tissue. Results are not significantly different between the two tissues. (D) Relative phosphorylated AMPKα protein concentration, this assays the amount of active AMPKα in the cell. Relative concentrations are not significantly different between the two tissues.

DISCUSSION

In the present study, I demonstrate that removal of the N2B region of titin significantly increases hysteresis. This was true in a rigorous battery of stretches covering physiological and extra-physiological conditions. In stretches from a well rested state, hysteresis increased an average of 4.4 fold in KO over WT tissue. During approximated physiological tandem triangle stretches, hysteresis starts out large, but quickly decreases to settle at a steady state value where KO had a 2-fold increase in hysteresis over WT tissue. Oxidation experiments in which part of the N2B-Us is cross-linked and mechanically 'hidden' support the hypothesis that the observed differences are due to the lack of the N2B-Us and not compensatory mechanisms. Below I discuss the results in detail.

Sources of Hysteresis in the Sarcomere

Of the possible sources of hysteresis, the two main types that are relevant to this study are viscosity from filament interaction and structural transitions within titin, particularly Ig domain unfolding, during stretching. Filament sliding viscosity occurs during the sarcomere stretch/release cycle and takes place between thin and thick filaments and thin and titin filaments. Hysteresis arises as sarcomeric filaments interact to oppose their sliding motion on both the ascending and descending limbs of the triangle stretch, increasing tension during the loading

cycle and decreasing it during the unloading cycle. These forces arise through non-specific electrostatic interactions between filaments or fluid motion through the dense protein filled sarcomere lattice. Ig domain unfolding-refolding also has the possibility to add large amounts of hysteresis due to the unique unfolding characteristics of Ig domains. The extra energy loss would come from work being done to dissociate the hydrogen bonds within the beta-barrel of the Ig domain that is not recovered during shortening.

To differentiate between interfilament and titin based hysteresis, a series of gelsolin thin filament extracted experiments were conducted. Most notable from these experiments is the difference between thin filament extracted and non thin filament extracted hysteresis of the initial stretch, where the tissue is rested. Hysteresis is greatly reduced initially in gelsolin-extracted muscle, but as it is preconditioned, this difference decreases as the tissue enters steady state. This suggests that the initial well-rested hysteresis has a large interfilament interaction component while the steady-state hysteresis relies more on sources of hysteresis intrinsic to titin. In summary, the steady-state hysteresis is remarkably insensitive to thin filament removal, and the source for this hysteresis is therefore likely to reside within titin.

In the case of the N2B KO, the sources of hysteresis within titin can only be the PEVK and tandem Ig segment. The PEVK consists of mostly random coil with interspersed short polyproline, PP, type II helices (Ma et al., 2001). For this murine model it is predicted that only a total of 6 residues may participate in PPII folding. (c.f. Ma et al., 2001) During stress, these secondary structures may unfold causing hysteresis. However, the hysteresis induced from PEVK PPII helix unfolding is expected to be small, as the L_c gain from this event is estimated at 0.42nm (6 residues *(0.38 nm - 0.31 nm)). On the other hand, Ig domain unfolding L_c gain is large enough to account for the increase in hysteresis seen in this study, ~30 nm per Ig domain unfolding event (Watanabe et al., 2002). Although it has been argued that Ig unfolding is unlikely to take place in WT titin (Trombitás et al., 1998; Helmes et al., 1999; Linke et al., 1998), unfolding of a few domains during stretch cannot be excluded and a few studies have given support to it (Minajeva et al., 2001; Erickson, 1994; Soteriou et al., 1993). Furthermore, former studies were carried out on well-rested muscle and the conclusions of those studies do not necessarily extrapolate to the physiological repeated stretch patterns in my work. Additionally, considering that deletion of the N2B element abolishes ~215 nm of extensibility within titin, unfolding is more likely to occur in the N2B deficient titin and can account for the increase in hysteresis. In fact, the maximum extension possible without Ig unfolding in the N2B KO is 2.26μm. The N2B element contributes ~215 nm to the L_c of the

extensible region (~200 nm Us and ~ 15 nm for its 3 Ig domains). The total L_c in the WT is 70 nm (PEVK), 160 nm (36 Ig domains in the tandem Ig segment * 4.5 nm/domain) and 215 for the N2B element = 445 nm. In the KO the CL is 70 + 160 = 230. 1.8 μm is the SL at which the extensible region has an end-to-end length of 0 nm (Trombitás et al., 1999). Thus in the KO, titin's extensibility will be exhausted at SL 2.26 μm (1.8μm + 2*0.23μm). However structural changes must happen at a shorter length, for if no structural changes would occur, passive tension is predicted to be infinite at this point by the worm like chain model (Watanabe et al., 2002). This is not seen in the results, and in fact passive tension approximates a linear relationship to SL at sarcomeric extensions around 2.26μm.

Another indication for Ig domain unfolding during physiological conditions can be obtained from the ratio between hysteresis and tension determined at different strain rates. Ig domain unfolding during stretch reduces peak tension (length of the domain increases from ~4.5 nm to ~35 nm and this decreases tension) while causing hysteresis. Thus increased unfolding during stretch will increase the hysteresis:tension ratio. Another insight that is needed is the stretch-speed dependence of unfolding. Because of the kinetic nature of unfolding, when stretch speed is increased, less time is spent at lower forces, lowering the probability that domains will unfold at those forces and allowing greater passive

tensions to develop (Rief et al., 1998). Combined, this leads to the prediction that if hysteresis is due to unfolding of Ig domains, the hysteresis:tension ratio should scale inversely with stretch speed. Note that hysteresis based on inter-filament viscosity will give rise to a hysteresis:tension ratio that varies in proportion to stretch speed, which is because the viscous forces act on both the loading and unloading curves, increasing peak tension while increasing hysteresis.

Results shown in Figure 13 indicate that in both WT and KO muscle, at all three strain amplitudes, as stretch speed increases the hysteresis:tension is reduced. Knowing Ig domain unfolding is required in triangle stretches to 2.3μm, the relationship between the hysteresis:tension ratio and stretch speed is used as a positive control relationship for Ig domain unfolding. The similarity between KO and WT tissue in the strain rate dependence against normalized hysteresis strongly suggests that Ig domain unfolding gives rise to hysteresis in both KO and WT muscle.

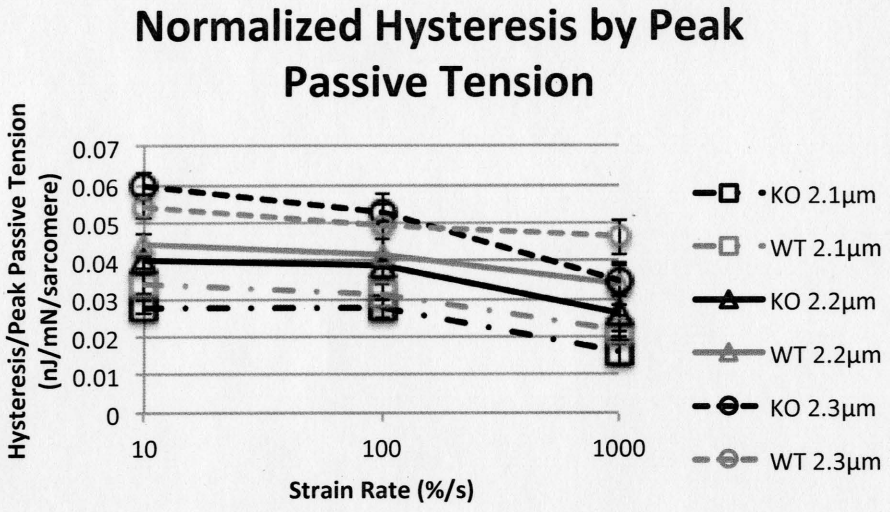

Figure 13
Hysteresis normalized by peak passive tension for each stretch. This normalization factor increases as tissue is stretched to longer SLs due to the fact that more Ig domains are unfolding and refolding during the stretch. This factor also decreases with increasing strain rate as the increased stretch speed lowers the probability for Ig domain unfolding even while passive tension increases.

Additionally, hysteresis recovery experiments also indicate that the mechanism behind hysteresis does not change in between WT and KO tissue. Hysteresis recovery time constants were quite similar in WT and KO tissue, 0.24 s^{-1} and 0.15 s^{-1} respectively. Furthermore, these values, while slightly slower, are on the same order of magnitude of recovery experiments in single molecule studies, 1 s^{-1} (Carrion-Vazquez et al., 1999). This difference could arise from the differences in stretch patterns. In my study I used a very asymmetric triangle stretch, while the single molecular work used simple symmetrical triangles, and the refolding

process could have already begun before it reached zero force, shortening the time for recovery. Additionally, in single molecular experiments, one molecule is allowed to refold in a huge volume of space. However, in the sarcomere molecular crowding may slow down refolding of titin domains, as seen in the results. The similarity between Ig domain recovery and recovery time constants in both WT and KO muscles further indicates Ig domain unfolding is not only happening in KO tissue but also WT tissue under physiological conditions.

N2B Removal Increases Hysteresis

To start understand how the removal of the N2B region of titin increases hysteresis, even at the same sarcomere length strain, attention must be given to the remaining portions of titin and how they operate without the N2B region. First, the remaining elements will experience more strain for the same whole tissue deformation in KO compared to WT tissue. As the entropic spring elements within titin experience greater strain, they will produce a larger restoring force and thus tension will increase within the cell. This is confirmed by my data in that deformations of smaller magnitude create larger tensions in KO compared to WT tissue. At a strain rate of 100%/s KO tissue stretched by 0.34μm had peak stresses of 27.6±5.7mN/mm^2 while WT tissue stretched a larger distance of 0.41μm had smaller peak stresses of 10.5±1.0mN/mm^2, p-value < 0.05. This

increase in tension in the KO will increase the probability of Ig domain unfolding (Rief et al., 1998), greatly increasing hysteresis.

N2B Deficiency Affects Slack Sarcomere Length

Removing such a large portion of titin will also adjust the slack SL in the KO model by the distance contributed by exon 49 under no forces. This distance is approximated by the unloaded mean-square separation for a worm like chain at low forces: $L_P\sqrt{L_C / L_P}$ (Nelson, P., 2008) plus the distance contributed by its Ig domains. This equates to roughly 12nm/half sarcomere ($0.65nm\sqrt{214.9nm / 0.65nm}$). Remarkably, this estimated reduction by 24nm/sarcomere is quite close to the measured difference of 30nm (1.89μm – 1.86μm, WT and KO respectively). A side effect of this reduction in slack SL is that stretches to the same SL will impose a slightly greater strain on KO tissue, as they start from a shorter position compared to WT, and may artificially inflate KO hysteresis. In my data, when KO tissue was stretched a shorter distance of 0.34μm it had 1.08±0.24nJ/mm²/sarcomere of hysteresis. While, when WT tissue was stretched a larger distance of 0.41μm it had significantly less hysteresis of 0.49±0.07nJ/mm²/sarcomere (WT vs. KO, p-value < 0.05). This indicates that removal of the N2B region of titin increases hysteresis much more than can be explained by exaggerated deformations caused by a decrease in slack SL.

N2B Removal Induced Energy Loss

I have shown both interfilament friction/viscous forces and Ig domain unfolding-refolding cause the initial rested hysteresis. During subsequent stretches interfilament forces contribute less and less toward hysteresis until the majority of hysteresis is contributed by Ig domain unfolding. The removal of the large compliant N2B-Us from titin causes a significant increase in Ig domain unfolding and thus hysteresis. To evaluate this reduction in hysteresis on a physiological scale, I calculated the percent of total energy consumption saved by incorporating the N2B-Us into cardiac titin. Initially, total energy consumption per beat was calculated by multiplying stroke volume, 31 μL (Janssen et al., 2002), by mean arterial pressure, 112 mmHg (Mattson, 2001), which after unit conversion approximates to 463 μJ ($3.1*10^{-8}$ m^3 * 14900 N/m^2) of mechanical energy exerted per beat for a normal working heart. This value is compared against the extra energy loss through an increase in hysteresis in KO over WT tissue. As seen in Table 1, first, hysteresis per beat was converted from units based on the sarcomere to hysteresis per volume by dividing by the slack sarcomere length, resulting in energy dissipation per volume per beat. Then, left ventricle (LV) muscle volume was approximated by multiplying the LV mass by the average mammalian muscle density (1.06 g/cm^3 (Urbanchek et al., 2001)). By multiplying hysteresis per volume by the LV muscle volume I was able to approximate energy loss per heart per beat, resulting in 18.8 μJ/beat and 26.2

μJ/beat for WT and KO tissue respectively. By dividing this increase in energy dissipation per beat, 26.2 μJ/beat – 18.8 μJ/beat = 7.9 μJ/beat, by total mechanical energy exerted, 463 μJ, I arrived at a ~2% increase in energy consumption per beat. I propose that this is functionally important and can have far reaching effects.

	hysteresis per beat		slack SL		energy disapation per volume per beat
WT	(320pJ/mm²/sarcomere)	/	1.89μm/sarcomere	=	169nJ/mm³/beat
KO	(650pJ/mm²/sarcomere)	/	1.86μm/sarcomere	=	349nJ/mm³/beat

	LV mass		muscle density		LV volume
WT	118mg	/ (	1.06g/cm³	) =	111mm³
KO	80mg	/ (	1.06mg/mm³	) =	75mm³

	energy disapation per volume per beat		LV volume		Energy loss
WT	(169nJ/mm³/beat	) *	111mm³	=	18.8μJ/beat
KO	(349nJ/mm³/beat	) *	75mm³	=	26.2μJ/beat

Table 1
Energy consumption calculations for both WT and KO muscle.

Cellular Impact

In this study I found that neither AMPK nor AMPK phosphorylation levels were significantly changed between WT and KO models. Thus the impact of increased hysteresis in the KO on this cellular metabolism regulator was minimal. In previous studies large stressors, on the order of 2 or 3-fold change in AMP:ATP ratio, were used to induce an increase in AMPK-P levels (Hawley et al., 1996, Choi et al., 2001, Ching et al., 2010). A possible explanation for the minimal changes in the data could be a result that the change in AMP:ATP ratio, induced by the removal of the N2B region, is below the threshold at which significant

changes in AMPK levels are seen. I speculate that stressing the mice, for example increasing the heart rate and contractility by beta-adrenergic stimulation such as occurs during the fight-or-flight response, might differentiate WT and KO AMPK responses.

In this study I used a reactive oxygen species (ROS), H_2O_2, to induce crosslinking within the N2B-Us to test whether the increase in hysteresis seen in the KO model is a result of the removal of the N2B region of titin. I found that cross-linking the N2B-Us not only increased passive tension (Grützner et al., 2009) but also increased hysteresis by a significantly greater percent in WT compared to KO muscle. As described in the introduction, this forms a 'half N2B KO model' free from genetic alteration complications. This data further confirms that titin, not interfilament interactions or friction, is the main source of hysteresis within the sarcomere.

It is likely that the N2B element performs multiple roles, including Phosphokinase A and G (PKA and PKG) signaling (Yamasaki 2002, Krüger and Linke, 2006) and anchoring signaling molecules (Matsumoto et al., 2005; Sheikh 2008). This study provides strong evidence for a mechanical role in increasing compliance and thereby reducing energy loss, which, due to its rhythmic activity pattern, is a critically important aspect of cardiac function.

REFERENCES

Helmes et al. Mechanically driven contour-length adjustment in rat cardiac titin's unique N2B sequence: titin is an adjustable spring. Circ Res (1999) vol. 84 (11) pp. 1339-52

Kellermayer et al. Complete unfolding of the titin molecule under external force. J Struct Biol (1998) vol. 122 (1-2) pp. 197-205

Wu et al. Changes in titin and collagen underlie diastolic stiffness diversity of cardiac muscle. J Mol Cell Cardiol (2000) vol. 32 (12) pp. 2151-62

Improta et al. Immunoglobulin-like modules from titin I-band: extensible components of muscle elasticity. Structure (1996) vol. 4 (3) pp. 323-37

Radke et al. Targeted deletion of titin N2B region leads to diastolic dysfunction and cardiac atrophy. Proc Natl Acad Sci USA (2007) vol. 104 (9) pp. 3444-9

Carling. The AMP-activated protein kinase cascade--a unifying system for energy control. Trends Biochem Sci (2004) vol. 29 (1) pp. 18-24

Grützner et al. Modulation of titin-based stiffness by disulfide bonding in the cardiac titin N2-B unique sequence. Biophys J (2009) vol. 97 (3) pp. 825-34

Watanabe et al. Molecular mechanics of cardiac titin's PEVK and N2B spring elements. J Biol Chem (2002) vol. 277 (13) pp. 11549-58

Lee et al. Calcium sensitivity and the Frank-Starling mechanism of the heart are increased in titin N2B region-deficient mice. J Mol Cell Cardiol (2010) vol. 49 (3) pp. 449-58

Granzier and Irving. Passive tension in cardiac muscle: contribution of collagen, titin, microtubules, and intermediate filaments. Biophys J (1995) vol. 68 (3) pp. 1027-44

Chung and Granzier. Contribution of titin and extracellular matrix to passive pressure and measurement of sarcomere length in the mouse left ventricle. J Mol Cell Cardiol (2011) vol. 50 (4) pp. 731-9

Noujaim et al. From mouse to whale: a universal scaling relation for the PR Interval of the electrocardiogram of mammals. Circulation (2004) vol. 110 (18) pp. 2802-8

Granzier et al. Titin elasticity and mechanism of passive force development in rat cardiac myocytes probed by thin-filament extraction. Biophys J (1997) vol. 73 (4) pp. 2043-53

King et al. Mouse intact cardiac myocyte mechanics: cross-bridge and titin-based stress in unactivated cells. J Gen Physiol (2011) vol. 137 (1) pp. 81-91

Kirk et al. Left ventricular and myocardial function in mice expressing constitutively pseudophosphorylated cardiac troponin I. Circ Res (2009) vol. 105 (12) pp. 1232-9

Vahebi et al. Functional effects of rho-kinase-dependent phosphorylation of specific sites on cardiac troponin. Circ Res (2005) vol. 96 (7) pp. 740-7

Slezak et al. Hydrogen peroxide changes in ischemic and reperfused heart. Cytochemistry and biochemical and X-ray microanalysis. Am J Pathol (1995) vol. 147 (3) pp. 772-81

Avner et al. H2O2 alters rat cardiac sarcomere function and protein phosphorylation through redox signaling. Am J Physiol Heart Circ Physiol (2010) vol. 299 (3) pp. H723-30

Janero and Hreniuk···. Hydrogen peroxide - induced oxidative stress to the mammalian heart - muscle cell (cardiomyocyte): Lethal peroxidative membrane injury. Journal of cellular ··· (1991)

Wijesekara et al. Adiponectin-induced ERK and Akt phosphorylation protects against pancreatic beta cell apoptosis and increases insulin gene expression and secretion. J Biol Chem (2010) vol. 285 (44) pp. 33623-31

Ma et al. Polyproline II helix is a key structural motif of the elastic PEVK segment of titin. Biochemistry (2001) vol. 40 (12) pp. 3427-38

Watanabe et al. Molecular mechanics of cardiac titin's PEVK and N2B spring elements. J Biol Chem (2002) vol. 277 (13) pp. 11549-58

Trombitás et al. Titin extensibility in situ: entropic elasticity of permanently folded and permanently unfolded molecular segments. J Cell Biol (1998) vol. 140 (4) pp. 853-9

Linke et al. Characterizing titin's I-band Ig domain region as an entropic spring. J Cell Sci (1998) vol. 111 (Pt 11) pp. 1567-74

Minajeva et al. Unfolding of titin domains explains the viscoelastic behavior of skeletal myofibrils. Biophys J (2001) vol. 80 (3) pp. 1442-51

Erickson. Reversible unfolding of fibronectin type III and immunoglobulin domains provides the structural basis for stretch and elasticity of titin and fibronectin. Proc Natl Acad Sci USA (1994) vol. 91 (21) pp. 10114-8

Soteriou et al. Titin folding energy and elasticity. Proc Biol Sci (1993) vol. 254 (1340) pp. 83-6

Trombitás et al. Molecular dissection of N2B cardiac titin's extensibility. Biophys J (1999) vol. 77 (6) pp. 3189-96

Rief et al. Elastically coupled two-level systems as a model for biopolymer extensibility. Phys. Rev. Letters (1998) vol. 81, pp. 4764 – 4767.

Carrion-Vazquez et al. Mechanical and chemical unfolding of a single protein: a comparison. Proc Natl Acad Sci USA (1999) vol. 96 (7) pp. 3694-9

Nelson, P. Biological Physics: Energy, Information, Life, Updated First Edition, W.H. Freeman and Company: New York, 2008; Chapter 9.2.1

Janssen et al. Chronic measurement of cardiac output in conscious mice. Am J Physiol Regul Integr Comp Physiol (2002) vol. 282 (3) pp. R928-35

Mattson. Comparison of arterial blood pressure in different strains of mice. Am J Hypertens (2001) vol. 14 (5 Pt 1) pp. 405-8

Urbanchek et al. Specific force deficit in skeletal muscles of old rats is partially explained by the existence of denervated muscle fibers. J Gerontol A Biol Sci Med Sci (2001) vol. 56 (5) pp. B191-7

Hawley et al. Characterization of the AMP-activated protein kinase kinase from rat liver and identification of threonine 172 as the major site at which it phosphorylates AMP-activated protein kinase. J Biol Chem (1996) vol. 271 (44) pp. 27879-87

Choi et al. The regulation of AMP-activated protein kinase by H(2)O(2). Biochem Biophys Res Commun (2001) vol. 287 (1) pp. 92-7

Ching et al. A role for AMPK in increased insulin action after serum starvation. Am J Physiol, Cell Physiol (2010) vol. 299 (5) pp. C1171-9

Yamasaki et al. Protein kinase A phosphorylates titin's cardiac-specific N2B domain and reduces passive tension in rat cardiac myocytes. Circ Res (2002) vol. 90 (11) pp. 1181-8

Krüger and Linke. Protein kinase-A phosphorylates titin in human heart muscle and reduces myofibrillar passive tension. J Muscle Res Cell Motil (2006) vol. 27 (5-7) pp. 435-44

Matsumoto et al. Functional analysis of titin/connectin N2-B mutations found in cardiomyopathy. J Muscle Res Cell Motil (2005) vol. 26 (6-8) pp. 367-74

Sheikh et al. An FHL1-containing complex within the cardiomyocyte sarcomere mediates hypertrophic biomechanical stress responses in mice. J Clin Invest (2008) vol. 118 (12) pp. 3870-80